Circulation Research

ORIGINAL RESEARCH

DWORF Extends Life Span in a PLN-R14del Cardiomyopathy Mouse Model by Reducing Abnormal Sarcoplasmic Reticulum Clusters

Nienke M. Stege, Tim R. Eijgenraam, Vivian Oliveira Nunes Teixeira, Anna M. Feringa, Elisabeth M. Schouten, Diederik W.D. Kuster, Jolanda van der Velden, Anouk H.G. Wolters, Ben N.G. Giepmans, Catherine A. Makarewich, Rhonda Bassel-Duby, Eric N. Olson, Rudolf A. de Boer, Herman H.W. Silljé

BACKGROUND: The p.Arg14del variant of the *PLN* (phospholamban) gene causes cardiomyopathy, leading to severe heart failure. Calcium handling defects and perinuclear PLN aggregation have both been suggested as pathological drivers of this disease. Dwarf open reading frame (DWORF) has been shown to counteract PLN regulatory calcium handling function in the sarco/endoplasmic reticulum (S/ER). Here, we investigated the potential disease-modulating action of DWORF in this cardiomyopathy and its effects on calcium handling and PLN aggregation.

METHODS: We studied a PLN-R14del mouse model, which develops cardiomyopathy with similar characteristics as human patients, and explored whether cardiac DWORF overexpression could delay cardiac deterioration. To this end, $R14^{\Delta/\Delta}$ (homozygous PLN-R14del) mice carrying the DWORF transgene ($R14^{\Delta/\Delta}DWORF^{Tg}$ [$R14^{\Delta/\Delta}$ mice carrying the DWORF transgene]) were used.

RESULTS: DWORF expression was suppressed in hearts of $R14^{\Delta/\Delta}$ mice with severe heart failure. Restoration of DWORF expression in $R14^{\Delta/\Delta}$ mice delayed cardiac fibrosis and heart failure and increased life span >2-fold (from 8 to 18 weeks). DWORF accelerated sarcoplasmic reticulum calcium reuptake and relaxation in isolated cardiomyocytes with wild-type PLN, but in $R14^{\Delta/\Delta}$ cardiomyocytes, sarcoplasmic reticulum calcium reuptake and relaxation were already enhanced, and no differences were detected between $R14^{\Delta/\Delta}$ and $R14^{\Delta/\Delta}DWORF^{Tg}$. Rather, DWORF overexpression delayed the appearance and formation of large pathogenic perinuclear PLN clusters. Careful examination revealed colocalization of sarcoplasmic reticulum markers with these PLN clusters in both $R14^{\Delta/\Delta}$ mice and human p.Arg14del PLN heart tissue, and hence these previously termed aggregates are comprised of abnormal organized S/ER. This abnormal S/ER organization in PLN-R14del cardiomyopathy contributes to cardiomyocyte cell loss and replacement fibrosis, consequently resulting in cardiac dysfunction.

CONCLUSIONS: Disorganized S/ER is a major characteristic of PLN-R14del cardiomyopathy in humans and mice and results in cardiomyocyte death. DWORF overexpression delayed PLN-R14del cardiomyopathy progression and extended life span in $R14^{\Delta/\Delta}$ mice, by reducing abnormal S/ER clusters.

GRAPHIC ABSTRACT: A graphic abstract is available for this article.

Key Words: cardiomyopathies ■ cell death ■ fibrosis ■ heart failure ■ sarcoplasmic reticulum

Meet the First Author, see p 964

A number of pathogenic mutations in the gene coding for PLN (phospholamban) have been identified that cause cardiomyopathy. The p.Arg14del pathogenic variant is the best described and most prevalent variant and may cause dilated cardiomyopathy or arrhythmogenic cardiomyopathy, often resulting in severe heart

Correspondence to: Herman H.W. Silljé, PhD, University Medical Center Groningen, University of Groningen, Antonius Deusinglaan 1, 9713AV, Groningen, The Netherlands. Email h.h.w.sillje@umcg.nl

Supplemental Material is available at https://www.ahajournals.org/doi/suppl/10.1161/CIRCRESAHA.123.323304.
For Sources of Funding and Disclosures, see page 1020.

Circulation Research is available at www.ahajournals.org/journal/res

Novelty and Significance

What Is Known?

- The p.Arg14del variant of the *PLN* (phospholamban) gene causes cardiomyopathy, leading to severe heart failure, which cannot be properly treated using current heart failure therapies.
- Mechanistic insights in disease development are required for a specific treatment, and a causal role in disease development has been suggested for the clustered perinuclear PLN protein.
- Dwarf open reading frame (DWORF) is a SERCA (sarco/endoplasmic reticulum Ca^{2+} ATPase) activator, with a function opposite to PLN and has shown to be cardioprotective in several murine heart failure models.

What New Information Does This Article Contribute?

- The current work shows that the characteristic dense perinuclear PLN structures in the PLN-R14del mouse model and human patients are composed of strongly clustered and disorganized cardiac sarco/endoplasmic reticulum.
- DWORF overexpression delays cardiac dysfunction and extends life span in a PLN-R14del cardiomyopathy mouse model.
- DWORF exerts its positive effects in PLN-R14del cardiomyopathy via the reduction of perinuclear PLN clustering and associated toxic sarco/endoplasmic reticulum disorganization, not via a change in sarcoplasmic reticulum calcium reuptake.

These data support sarco/endoplasmic reticulum disorganization as a detrimental mechanism in the development of PLN-R14del cardiomyopathy. Preventing structural sarco/endoplasmic reticulum alterations by DWORF overexpression or by other interventions could be a promising therapeutic strategy in this disease.

Nonstandard Abbreviations and Acronyms

ATL3	atlastin-3
DWORF	dwarf open reading frame
HF	heart failure
HRC	histidine-rich calcium binding protein
LVEF	left ventricular ejection fraction
PLN	phospholamban
R14$^{\Delta/\Delta}$	homozygous PLN-R14del
R14$^{\Delta/\Delta}$DWORF^{Tg}	R14$^{\Delta/\Delta}$ mice carrying the DWORF transgene
S/ER	sarco/endoplasmic reticulum
SERCA	sarco/endoplasmic reticulum Ca^{2+} ATPase
SR	sarcoplasmic reticulum
WT	wild-type

failure (HF) with characteristic perinuclear PLN aggregates.[1,2] So far, no specific treatment for this cardiomyopathy is available, and heart transplantation often is needed as a last resort.

PLN is a small cardiac-specific protein that localizes to the sarcoplasmic reticulum (SR) membrane, where it negatively regulates the reuptake of cytosolic calcium ions (Ca^{2+}) into the SR via its interaction with the SERCA (sarco/endoplasmic reticulum Ca^{2+}-ATPase).[3] Calcium handling studies have shown different effects of PLN-R14del on SERCA regulation, and the precise contribution of dysfunctional SERCA regulation in the pathology of this disease is still under debate.[4–8] Additionally, functions of PLN have been attributed to nuclear and mitochondrial mechanisms,[9,10] suggesting more complex PLN interactions and function. A recent study using human induced pluripotent stem cell–derived cardiac tissues suggested impairment of the endoplasmic reticulum/mitochondria compartment as a novel disease mechanism underlying PLN-R14del cardiomyopathy.[10] Interestingly, human PLN-R14del cardiomyopathy is characterized by the presence of dense perinuclear PLN protein aggregates in cardiomyocytes.[11] Furthermore, in a mouse model of PLN-R14del cardiomyopathy, clustered perinuclear PLN protein was identified and was consistently found to be the first pathological sign, preceding the onset of cardiac dysfunction, suggesting a causal role.[12,13] So far, the exact nature of the perinuclear PLN aggregates in PLN-R14del cardiomyopathy is unknown, but the strong association with disease development warrants further investigations.

A recently discovered SR localized micropeptide, termed dwarf open reading frame (DWORF), with a function opposite to PLN, was strongly downregulated in humans and mice with HF.[14–16] Using a transgenic mouse line, DWORF overexpression was shown to improve SERCA-mediated calcium reuptake and prevent HF in the MLP-KO (muscle LIM protein knock out) dilated cardiomyopathy mouse model.[17] In addition, DWORF

overexpression improved ventricular function and reduced cardiac dilation in a mouse model of myocardial infarction.[18] These studies have thus shown that DWORF overexpression is cardioprotective in HF from genetic but also common etiology, most likely via enhanced calcium reuptake. Whether DWORF affords cardioprotection in PLN-R14del cardiomyopathy, with its characteristic dense perinuclear PLN clusters, is unknown.

A mouse model that recapitulates the human PLN-R14del pathological phenotype has been described.[12] Mice harboring the heterozygous mutation develop disease characteristics at around 18 months of age, which is similar to what clinically is observed in humans where age of onset often is around 40 to 50 years. Mice harboring both pathogenic PLN-R14del alleles (homozygous, $R14^{\Delta/\Delta}$) showed an enhanced and accelerated phenotype developing in 4 to 8 weeks, while standard HF treatments could not attenuate disease progress, again in accordance with clinical observations.[12]

Here, we investigated the effect of DWORF overexpression in PLN-R14del cardiomyopathy. In particular, $DWORF^{Tg}$ mice were crossbred with PLN-$R14^{\Delta/\Delta}$ mice to generate $R14^{\Delta/\Delta}DWORF^{Tg}$ ($R14^{\Delta/\Delta}$ mice carrying the DWORF transgene) mice. We found that overexpression of DWORF in PLN-$R14^{\Delta/\Delta}$ mice reduced PLN-R14del–induced sarco/endoplasmic reticulum (S/ER) cluster formation, improved cardiac function, and extended life span.

METHODS

Data Availability

The data, methods, and study materials used to conduct the research are available from the corresponding authors on reasonable request. Expanded Methods are available in the Supplemental Material; also please see the Major Resources Table in the Supplemental Material.

Animals

Animal studies were approved by the Central Committee of Animal experiments (CCD; license number AVD1050020199105) and the animal ethical committee of the University of Groningen (permit numbers IVD199105-01-003, IVD199105-01-010, and IVD199105-01-022 for the current study; IVD1583-02-001 for DWORF gene expression in 3- to 7-week-old $R14^{\Delta/\Delta}$ [homozygous PLN-R14del] mice; and DEC6827A, DEC6920A, and IVD16487-03-01 for the samples we used from the study by Du et al[19]) and conformed with the guidelines from the Directive 2010/63/EU of the European Parliament on the protection of animals used for scientific purposes and reported following the Animal Research: Reporting of In Vivo Experiments (ARRIVE) guidelines.[20]

Study Design

To determine the effect of DWORF overexpression on the development of PLN-R14del cardiomyopathy, the $DWORF^{Tg}$ mice were crossed with the PLN-$R14^{\Delta/\Delta}$ mouse model ($R14^{\Delta/\Delta}DWORF^{Tg}$). Mice were assigned to the experimental groups by their genotype. The life span of $R14^{\Delta/\Delta}$ mice with and without DWORF overexpression (male and female, in total n=7–9 per group) was determined. Furthermore, cardiac function of these mice and their wild-type (WT; transgene negative) littermates was evaluated using echocardiography at 4, 6, 10, 14, and 18 weeks of age. In addition, ECG and several histological and molecular analyses were performed at 3, 5, 7, and 18 weeks of age (both male and female, mice of each genotype were randomly assigned to the different experimental time points, per group n=3, 8, 10, and 8, respectively). $R14^{\Delta/\Delta}DWORF^{Tg}$ mice that reached the humane end point (which occurred between 17 and 20 weeks of age) and their 22-week-old WT controls will be referred to as 18 weeks of age.

Echocardiography

Two-dimensional transthoracic echocardiography measurements were performed using the Vevo 3100 system with a 40-MHz MXX550D linear array transducer (FUJIFILM VisualSonics, Canada) as described previously.[21] During imaging, mice were anaesthetized with a mixture of oxygen and isoflurane (2.5%). Cardiac dimensional and functional parameters were determined using Vevo LAB software (version 3.2.6; FUJIFILM VisualSonics). Data acquisition and analysis were conducted in accordance with the recommendations of the European Society of Cardiology Working Group on Myocardial Function[22] and were performed in a blinded fashion.

Surface Electrocardiography

Lead II configuration ECG recordings were acquired on anesthetized mice (2.5% isoflurane mixed with oxygen), by a previously reported procedure.[12] Subdermal needle electrodes were connected to a PowerLab 8/30 data acquisition device (model ML870; ADInstruments, New Zealand) and an animal Bio Amp biological potential amplifier (model ML136; ADInstruments), which transferred recordings to LabChart Pro software (version 8; ADInstruments). The ECG analysis module was used for data analysis.

Histological Analysis

Heart tissue was fixed overnight in 4% buffered formaldehyde solution (4% formalin; Klinipath, the Netherlands). Afterward, tissues were dehydrated using an automated system (Leica TP1020; Leica Microsystems, Germany), embedded in paraffin (Klinipath), and cut into 4-µm-thick sections. Slides were deparaffinized before proceeding with the subsequent staining protocol. Staining protocols are available in the Supplemental Material, and the antibodies used are presented in Table S1.

Western Blot Analysis

Radioimmunoprecipitation assay lysis buffer was used to isolate proteins from snap-frozen left ventricular tissue as described previously.[12] Quantification was performed using ImageJ software (National Institutes of Health),[23] and the measurements of the protein of interest were corrected for the measured total amount of loaded protein that was determined using the Revert 700 Total Protein Stain (LI-COR Biosciences, NE). The calculated values were presented as a fold change compared with the age-matched control group. The primary and secondary antibodies that were used are presented in Table S3.

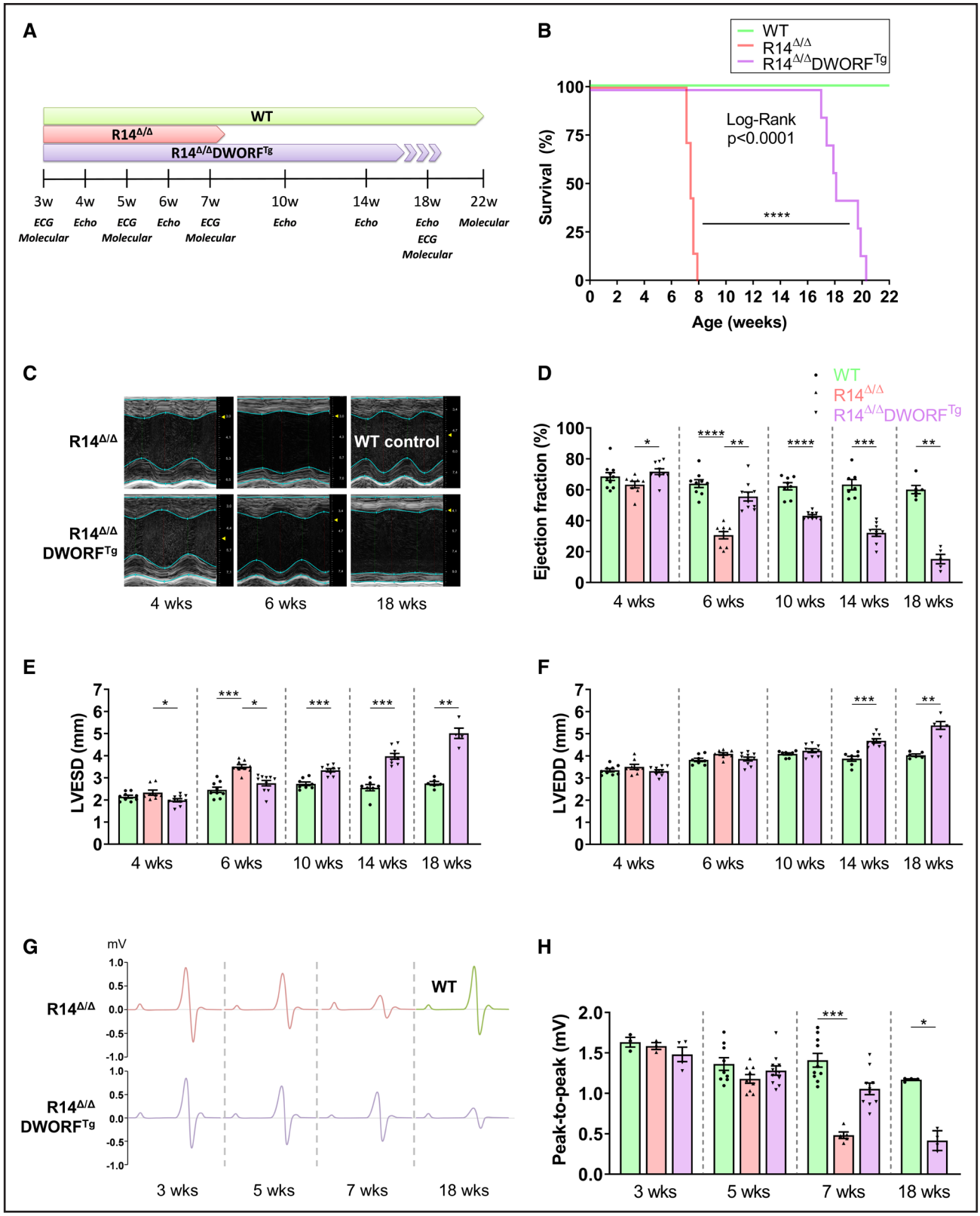

Figure 1. Dwarf open reading frame (DWORF) overexpression extended life span and inhibited cardiac impairment in R14$^{\Delta/\Delta}$ (homozygous PLN-R14del) mice.

A, Overview of the experimental design. **B**, Survival curve of wild-type (WT), R14$^{\Delta/\Delta}$, and R14$^{\Delta/\Delta}$DWORF^{Tg} (R14$^{\Delta/\Delta}$ mice carrying the DWORF transgene) mice, expressed as a percentage over time (n=7–9 per group). Significance was examined by the log-rank (Mantel-Cox) test. Representative (average based) serial M-mode echocardiographic images of the left ventricle (LV; **C**) with quantification of the ejection fraction (**D**), end-systolic diameter (LVESD; **E**), and end-diastolic diameter (LVEDD; **F**). Group sizes for echo data are n=8 to 10, (*Continued*)

ORIGINAL RESEARCH

Calcium Transient and Contraction Measurements in Isolated Adult Mouse Cardiomyocytes

Cardiomyocytes were isolated from WT, R14$^{\Delta/\Delta}$,and R14$^{\Delta/\Delta}$DWORF^{Tg} mice at 3 or 6 weeks of age (n=4 per genotype) using the protocol of Ackers-Johnson et al.[24] An IonOptix Calcium and Contractility System (IonOptix Corporation, MA) was used to measure calcium transients and video-based sarcomere length in Fura-2–loaded cardiomyocytes under pacing conditions (IonOptix MyoPacer; 2 Hz, 4 ms pulse duration, 20 V) at 37 °C. Calcium and contractility data were analyzed using CytoSolver, a cloud-based analysis program of IonOptix.

Electron Microscopy

Electron microscopy with PLN quantum dot immunolabeling was performed as reported previously.[25,26]

Statistical Analyses

All data are presented as mean±SEM, with the exception of calcium transient and contraction data that are presented as truncated violin plots (median and quartiles are indicated by lines). Nonparametric tests were performed because of small group sizes. Therefore, the Mann-Whitney *U* test was performed for comparisons between 2 groups and the Kruskal-Wallis test followed by Dunn post hoc test for multigroup comparisons. For statistical analysis of survival curves, a log-rank test was performed. Since individual cardiomyocytes instead of individual animals were plotted for calcium transient and contraction data, a hierarchical cluster analysis using customized R software (version 4.3.1) was applied according to the method described by Sikkel et al,[27] after log transformation of the data because of non-normal distribution. All other statistical analyses were performed using GraphPad Prism (version 8.4.2; GraphPad Software, MA). $P<0.05$ was considered statistically significant. Additional details on all statistical tests performed can be found in a supplemental statistical report.

RESULTS

DWORF Overexpression Extended Life Span and Improved Cardiac Function in R14$^{\Delta/\Delta}$ Mice

DWORF has been shown to be downregulated in HF in both mice and humans.[14,17] We confirmed downregulation of cardiac DWORF gene expression in our PLN-R14del cardiomyopathy mouse model (Figure S1A). At end-stage disease, DWORF gene expression levels in PLN-R14del mice were significantly lower than in mice with myocardial ischemia reperfusion injury and in mice that underwent myocardial infarction (Figure S1B). Since DWORF and PLN have been reported to have opposite functions, we investigated whether elevated DWORF levels could have beneficial effects against PLN-R14del cardiomyopathy development. To this aim, DWORF^{Tg} and PLN-R14$^{\Delta/\Delta}$ mice were crossed (R14$^{\Delta/\Delta}$DWORF^{Tg}) and an elevated DWORF protein level in the R14$^{\Delta/\Delta}$DWORF^{Tg} strain was confirmed by Western blot analysis (Figure S1C and S1D). To determine the effect of DWORF overexpression on the development of PLN-R14del cardiomyopathy, cardiac function and cardiac histological and molecular changes were evaluated over time and life span was determined, as outlined in Figure 1A.

A striking extension of life span was achieved by DWORF overexpression in PLN-R14$^{\Delta/\Delta}$ mice. While R14$^{\Delta/\Delta}$ mice have a limited life span of ≈8 weeks, this was substantially prolonged to 17 to 20 weeks by DWORF overexpression (R14$^{\Delta/\Delta}$DWORF^{Tg}; Figure 1B). Moreover, at 6 weeks of age, cardiac function (left ventricular ejection fraction [LVEF]) of R14$^{\Delta/\Delta}$ mice was already severely impaired (LVEF <35%), whereas cardiac function of R14$^{\Delta/\Delta}$DWORF^{Tg} mice was still preserved (LVEF >55%) and comparable to WT (Figure 1C and 1D). At about 10 weeks of age, cardiac dysfunction was detected in the R14$^{\Delta/\Delta}$DWORF^{Tg} mice, and at 14 weeks, the LVEF was as severely impaired as in the 6-week R14$^{\Delta/\Delta}$ group. Other parameters of PLN cardiomyopathy were also attenuated by DWORF overexpression, including the end-systolic diameter (Figure 1E), a measure of cardiac dilatation during contraction. The end-diastolic diameter did not significantly change in R14$^{\Delta/\Delta}$ mice and in R14$^{\Delta/\Delta}$DWORF^{Tg} mice at 6 weeks, but it increased in R14$^{\Delta/\Delta}$DWORF^{Tg} mice starting at 14 weeks of age (Figure 1F). Since low-voltage ECGs are a hallmark of PLN-R14del cardiomyopathy in patients, the ECG potential was quantified by the peak-to-peak amplitude at different time points in this study. At 7 weeks of age, ECG peak-to-peak amplitude was significantly reduced in the R14$^{\Delta/\Delta}$ group (0.48±0.04 mV; $P<0.05$ versus WT, 1.41±0.27 mV), whereas ECG potentials were preserved in R14$^{\Delta/\Delta}$DWORF^{Tg} mice (1.06±0.07 mV; Figure 1G and 1H). At 18 weeks of age, the amplitude of the R14$^{\Delta/\Delta}$DWORF^{Tg} group was decreased to 0.42±0.12 mV as well. The quantification of P, R, and S amplitudes is displayed in Figure S2. Together, these results indicate that DWORF overexpression delayed cardiac impairment in R14$^{\Delta/\Delta}$ mice, thereby extending the life span of these mice.

DWORF Overexpression Delayed Cardiac Remodeling in R14$^{\Delta/\Delta}$ Mice

The positive effects of DWORF on the development of HF were also validated at the molecular level. The well-documented increases in gene expression of the HF marker *Nppa* (ANP [atrial natriuretic peptide]) and the ratio *Myh7*/*Myh6* (myosin heavy chain 7, encoding β-myosin heavy chain; myosin heavy chain 6, encoding

Figure 1 Continued. except for age 18 weeks for which n=5 to 7. **G**, Schematic representation of ECG tracings taken at different time points. The average from 1-minute ECG recordings of multiple mice was used. The *x* axis per ECG complex has a duration of 90 ms. **H**, Quantification of the ECG peak-to-peak amplitude (n=3–4 at 3 wk, n=9–11 at 5 wk, n=5–10 at 7 wk, and n=4 at 18 wk). WT in green, R14$^{\Delta/\Delta}$ in red, and R14$^{\Delta/\Delta}$DWORF^{Tg} in purple. Significance was examined by Kruskal-Wallis with Dunn multiple comparisons test or the Mann-Whitney *U* test when 2 groups were compared. *$P<0.05$, **$P<0.01$, ***$P<0.001$, ****$P<0.0001$.

α-myosin heavy chain) in R14$^{\Delta/\Delta}$ mice were significantly reduced by DWORF overexpression at both 5 and 7 weeks of age (Figure 2A and 2B). For both *Nppa* and the ratio *Myh7/Myh6*, an expression level comparable to 7-week-old R14$^{\Delta/\Delta}$ mice was reached in R14$^{\Delta/\Delta}$DWORF^{Tg} mice at 18 weeks of age. Moreover, elevation of gene expression of the fibrotic markers *Col1a1* (collagen type I α1 chain) and *Lgals3* (galectin-3) was delayed by overexpression of DWORF in PLN-R14$^{\Delta/\Delta}$ mice (Figure 2C and 2D).

Consistent with these findings, histological analyses revealed that fibrosis occurred significantly slower in R14$^{\Delta/\Delta}$DWORF^{Tg} mice as compared with R14$^{\Delta/\Delta}$ mice (2.6±0.4% versus 12.5±1.0% at 7 weeks of age; $P<0.05$; WT, 1.2±0.2%; Figure 2E and 2F). At 18 weeks of age, cardiac fibrosis was elevated in the R14$^{\Delta/\Delta}$DWORF^{Tg} group as well (12.1±0.4%; $P<0.05$ versus WT).

DWORF Overexpression Did Not Alter Calcium Reuptake in R14$^{\Delta/\Delta}$ Mice

To investigate calcium handling and sarcomere contraction and relaxation, mouse cardiomyocytes were isolated at 3 weeks of age, before disease onset. Calcium

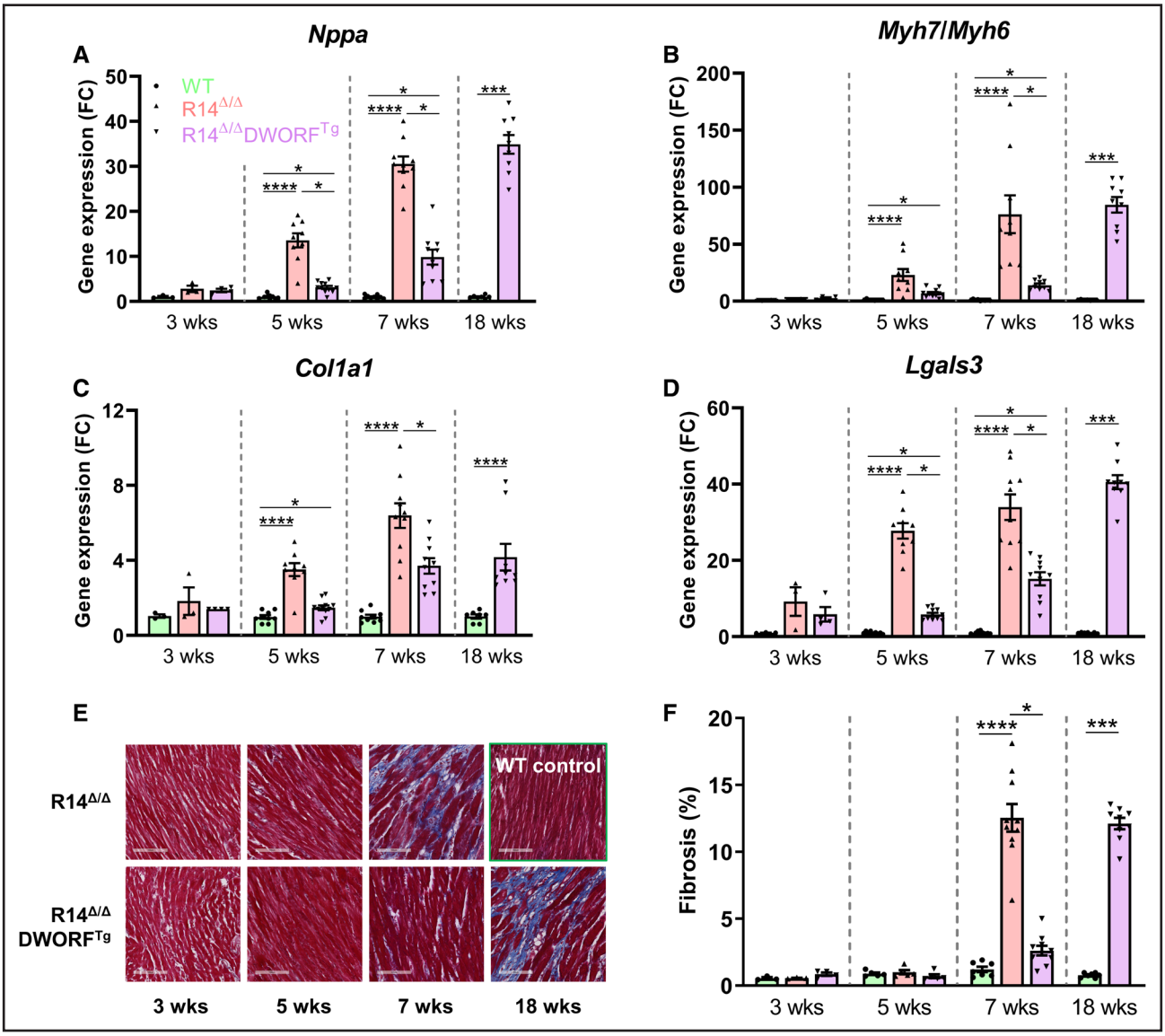

Figure 2. Dwarf open reading frame (DWORF) overexpression inhibited pathological gene expression and cardiac fibrosis in R14$^{\Delta/\Delta}$ (homozygous PLN-R14del) mice.

Relative left ventricular (LV) gene expression of the heart failure (HF) marker *Nppa* (**A**), the *Myh7/Myh6* ratio (**B**), and fibrotic markers *Col1a1* (**C**) and *Lgals3* (**D**), measured by quantitative PCR (qPCR) and displayed as a fold change (FC) difference to age-matched wild-type (WT) controls (n=3 at 3 wk, n=9 at 5 wk, n=10 at 7 wk, and n=8–9 at 18 wk). **E**, Representative (average based) Masson trichrome–stained cardiac tissue sections (scale bar, 100 µm). **F**, Quantification of cardiac fibrosis (n=3 at 3 wk, n=5 at 5 wk, n=10 at 7 wk, and n=8–9 at 18 wk). WT in green, R14$^{\Delta/\Delta}$ in red, and R14$^{\Delta/\Delta}$DWORF^{Tg} (R14$^{\Delta/\Delta}$ mice carrying the DWORF transgene) in purple. Significance was examined by Kruskal-Wallis with Dunn multiple comparisons test or the Mann-Whitney *U* test when 2 groups were compared. *$P<0.05$, ***$P<0.001$, ****$P<0.0001$.

transient investigations (τ, time to 80% decay of calcium peak, and relaxation velocity) showed accelerated relaxation in both R14$^{\Delta/\Delta}$ and R14$^{\Delta/\Delta}$DWORF^{Tg} compared with WT and no difference between R14$^{\Delta/\Delta}$ and R14$^{\Delta/\Delta}$DWORF^{Tg} (Figure 3A and 3B). In agreement with previous data,[14] DWORF^{Tg} in a WT PLN background significantly decreased τ (Figure S3A and S3B), but DWORF overexpression had no additional effect in R14$^{\Delta/\Delta}$ cardiomyocytes, because of the already low τ value in R14$^{\Delta/\Delta}$. No significant differences in calcium amplitudes were observed between cardiomyocytes from the different genotypes (Figure 3A; Table S4). Consistent

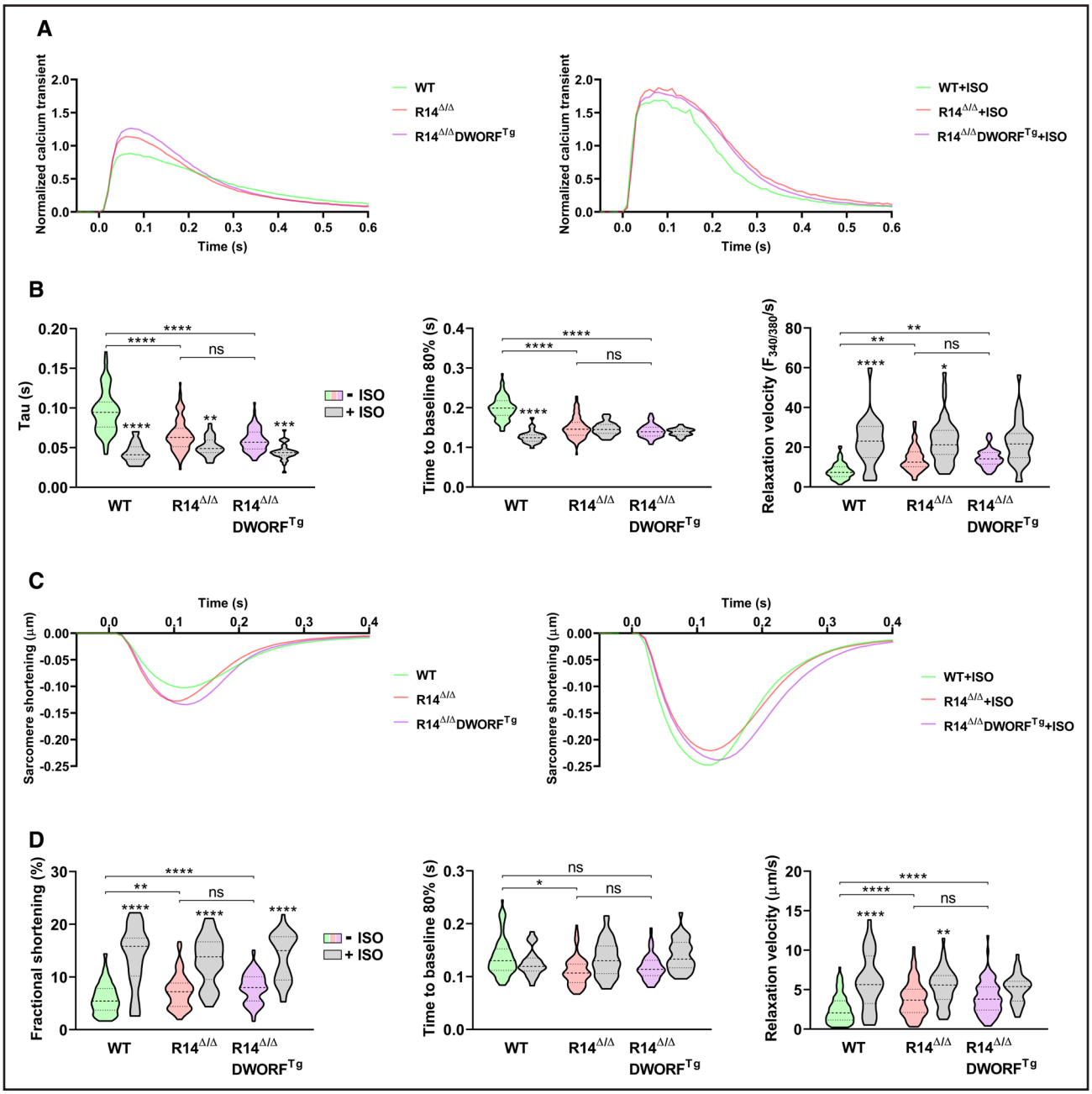

Figure 3. Dwarf open reading frame (DWORF) overexpression did not alter calcium handling in R14$^{\Delta/\Delta}$ (homozygous PLN-R14del) mice.

A, Normalized calcium transients under pacing conditions with and without isoproterenol (ISO) stimulation. **B**, decay time constant (τ), time to reduce systolic calcium level by 80% (T_{80}), and relaxation velocity. **C**, Normalized pacing-induced sarcomere contraction-relaxation curves with and without ISO stimulation. **D**, Fractional shortening, time to reach 80% of the diastolic sarcomere length after systole, and relaxation velocity. Calcium and contraction measurements were simultaneously performed in isolated adult mouse cardiomyocytes from 3-week-old wild-type (WT), R14$^{\Delta/\Delta}$, and R14$^{\Delta/\Delta}$DWORF^{Tg} (R14$^{\Delta/\Delta}$ mice carrying the DWORF transgene) mice (–ISO: n=60–100 cells from 4 mice per group; +ISO: n=30–40 cells from 4 mice per group). ISO condition was compared with the untreated matched genotype. Significance was examined by hierarchical cluster analysis using ANOVA with Bonferroni correction. *P<0.05, **P<0.01, ***P<0.001, ****P<0.0001.

with calcium observations, sarcomere relaxation velocity was significantly enhanced in both 3-week-old R14$^{\Delta/\Delta}$- and R14$^{\Delta/\Delta}$DWORF^{Tg}-derived cardiomyocytes compared with WT, and there was no difference between R14$^{\Delta/\Delta}$ and R14$^{\Delta/\Delta}$DWORF^{Tg} in sarcomere relaxation time and relaxation velocity (Figure 3C and 3D). Beneficial effects by DWORF overexpression could also not be explained by an increase in sarcomere fractional shortening (Figure S3C and S3D) since there was no significant difference in fractional shortening between R14$^{\Delta/\Delta}$DWORF^{Tg} and R14$^{\Delta/\Delta}$ cardiomyocytes (Figure 3C and 3D). β-Adrenergic stimulation with isoproterenol enhanced contraction and relaxation in all genotypes but had a reduced effect on relaxation parameters in R14$^{\Delta/\Delta}$DWORF^{Tg} and R14$^{\Delta/\Delta}$ cardiomyocytes, which is in accordance with the improved baseline values in these genotypes (Figure 3A through 3D). Cardiomyocytes isolated at 6 weeks of age, when disease is already present, were also investigated. Cardiomyocyte isolation was more challenging for the 6-week R14$^{\Delta/\Delta}$ hearts, and yields of viable cardiomyocytes were consistently lower (about 8-fold lower as compared with WT). Data from these apparent more vulnerable cardiomyocytes, which at this age also have become hypertrophic (Figure S4A), should, therefore, be interpreted with caution. Nevertheless, even though sarcomere data depict reduced quality of the 6-week-old R14$^{\Delta/\Delta}$ isolated cardiomyocytes, calcium transients at this age are similar to the findings at 3 weeks of age (Figure S4B through S4E). Together, the above results demonstrate that calcium reuptake is accelerated in R14$^{\Delta/\Delta}$ mice and indicate that the mechanism by which DWORF inhibits disease progression R14$^{\Delta/\Delta}$ mice is unrelated to a change in calcium handling.

DWORF Overexpression Inhibited the Formation of Characteristic PLN Aggregates in R14$^{\Delta/\Delta}$ Mice

Since hearts of PLN-R14del patients and R14$^{\Delta/\Delta}$ mice display characteristic dense perinuclear PLN localization, the effect of DWORF on this phenomenon was evaluated. While perinuclear PLN accumulation was present in almost all cardiomyocytes of R14$^{\Delta/\Delta}$ mice at 7 weeks of age, R14$^{\Delta/\Delta}$DWORF^{Tg} mice had only a few PLN aggregate positive cardiomyocytes (Figure 4A and 4B). Strikingly, even at 18 weeks of age, only a limited number of cardiomyocytes showed this characteristic PLN mislocalization. This demonstrates that DWORF overexpression is associated with less perinuclear PLN mislocalization. In correspondence with previous data,[12,28] there was a trend toward decreased PLN protein levels in 7-week-old R14$^{\Delta/\Delta}$ mice compared with WT (P=0.07), and the slower electrophoretic PLN phosphorylated forms were absent in R14$^{\Delta/\Delta}$ mice (Figure 4C and 4D). PLN protein levels were comparable between R14$^{\Delta/\Delta}$ and R14$^{\Delta/\Delta}$DWORF^{Tg} mice at both 7 and 18 weeks of age (Figure 4C and 4D), even though fewer perinuclear PLN clusters were present in R14$^{\Delta/\Delta}$DWORF^{Tg} mice (Figure 4A and 4B). Thus, the difference in PLN accumulation was not a result of altered PLN protein expression. Together this indicates that perinuclear PLN accumulation is a key pathological process in PLN-R14del cardiomyopathy and its reduction can delay disease development.

Dense PLN Perinuclear Structures Are Comprised of Mislocalized S/ER

Despite the pathological relevance of PLN accumulation in PLN-R14del cardiomyopathy, little is known about the composition of these perinuclear PLN clusters. To obtain more information about the ultrastructure of this clustered PLN, electron microscopy was performed on left ventricular tissue from 7-week-old R14$^{\Delta/\Delta}$ mice, 18-week-old R14$^{\Delta/\Delta}$DWORF^{Tg} mice, and WT controls. Using quantum dot labeling of an anti-PLN antibody, PLN clusters were visualized in the electron microscopy samples.

In R14$^{\Delta/\Delta}$ mice, highly dense clusters of labeled PLN were mainly present in the perinuclear region (Figure 5A, PLN clusters outlined in red and nucleus outlined in blue), which corresponds with the initial description of perinuclear localization of PLN aggregates in PLN-R14del patient material.[11,29] Importantly, the clustered PLN labeling was present in large membrane-like structures (Figure 5B). These structures were also present in 18-week-old R14$^{\Delta/\Delta}$DWORF^{Tg} mice (Figure 5C and 5D) but were not as abundant as compared with R14$^{\Delta/\Delta}$ mice, in agreement with fluorescent imaging (Figure 4A and 4B). In WT hearts, no PLN clusters were detected, but labeled PLN was distributed throughout the cell and localization to organized S/ER structures was observed (Figure 5E and 5F). The clustered membrane-like structures in R14$^{\Delta/\Delta}$ cardiac tissue did not correspond with vesicles like autophagosomes, which have double layer membranes, or lysosomes, which are spherical vesicles. Since PLN is a transmembrane protein anchored in the SR membrane, these large membrane structures could be disorganized clusters of the S/ER membrane.

To investigate the organization of the S/ER in cardiomyocytes from R14$^{\Delta/\Delta}$ mice, immunofluorescence microscopy was performed on left ventricular tissue from R14$^{\Delta/\Delta}$ and WT mice to visualize PLN together with other S/ER resident proteins. In contrast to the equal distribution throughout the cardiomyocytes observed in WT mice (Figure S5), clustering of the longitudinal tubular SR resident proteins SERCA2, HRC (histidine-rich calcium binding protein), and calnexin was observed in cardiac tissue from R14$^{\Delta/\Delta}$ mice (Figure 6). Moreover, these SR resident proteins colocalized with PLN at the perinuclear clusters (Figure 6). The structural endoplasmic reticulum protein ATL3 (atlastin-3) clustered and colocalized with the PLN clusters as well (Figure 6). In contrast, the sarcomere

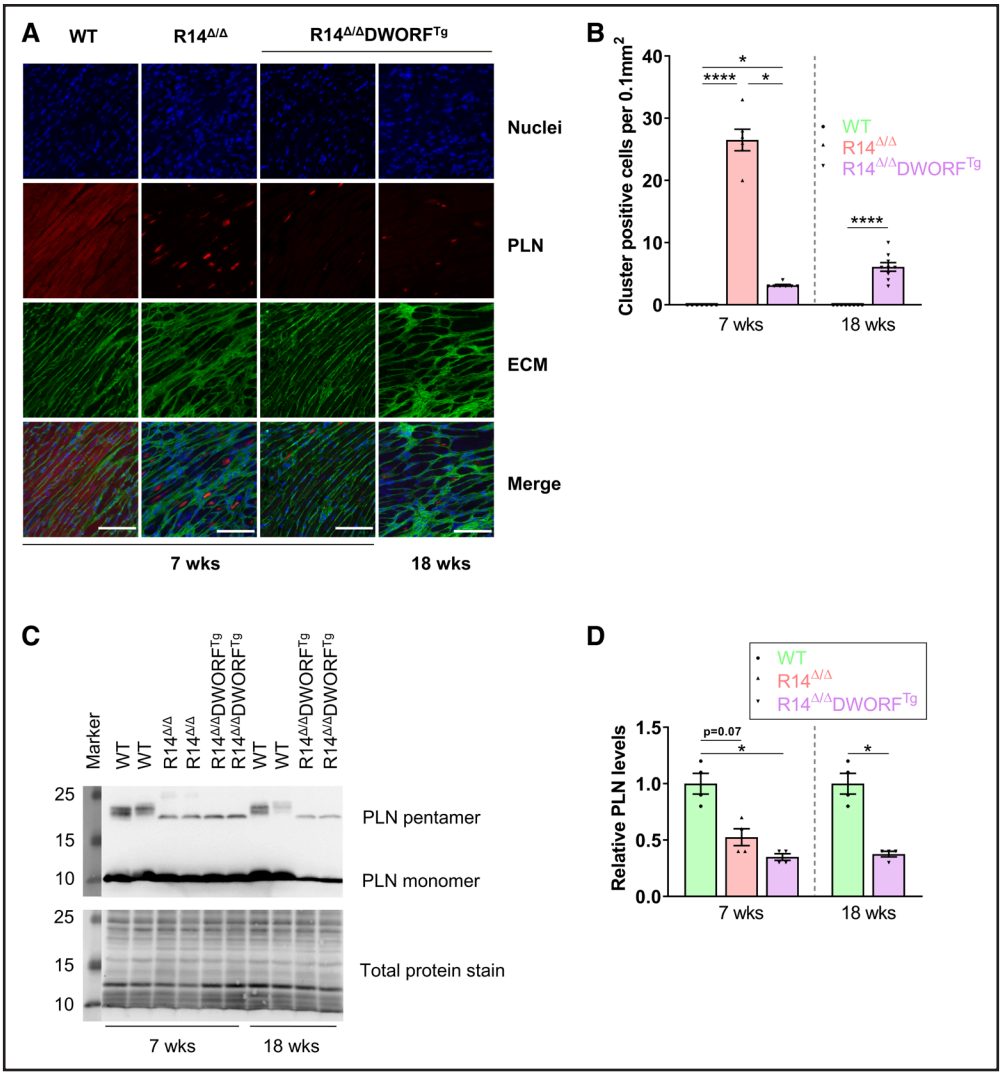

Figure 4. Inhibition of PLN (phospholamban) cluster formation accounts for the beneficial effects of dwarf open reading frame (DWORF) in R14$^{\Delta/\Delta}$ (homozygous PLN-R14del) mice.

A, Representative (average based) immunofluorescence (IF) staining of PLN (red), together with wheat germ agglutinin (WGA) staining the extracellular matrix (green) and 4',6-diamidino-2-phenylindole (DAPI) staining the nuclei (blue) in left ventricular (LV) tissue sections of wild-type (WT), R14$^{\Delta/\Delta}$, and R14$^{\Delta/\Delta}$DWORF^{Tg} (R14$^{\Delta/\Delta}$ ice carrying the DWORF transgene) mice of 7 or 18 weeks of age (scale bar, 100 µm). **B**, PLN cluster positive cardiomyocyte count per 0.1 mm^2 (n=6–9 per group). **C**, Representative (average based) Western blot images of PLN protein levels in LVs of WT, R14$^{\Delta/\Delta}$, and R14$^{\Delta/\Delta}$DWORF^{Tg} mice of 7 or 18 weeks of age. **D**, Total PLN protein level quantified and shown as fold change compared with age-matched WT mice (n=4 per group). WT in green, R14$^{\Delta/\Delta}$ in red, and R14$^{\Delta/\Delta}$DWORF^{Tg} in purple. Significance was examined by Kruskal-Wallis with Dunn multiple comparisons test or the Mann-Whitney *U* test when 2 groups were compared. *P<0.05, ****P<0.0001.

protein troponin and mitochondrial protein Tom20 (translocase of outer mitochondrial membrane 20) were distributed throughout the cell, as in WT mice (Figure S5), and did not colocalize with the PLN clusters in R14$^{\Delta/\Delta}$ mice (Figure 6). Although fewer clusters were present at 3 weeks of age, when present, SERCA2, HRC, calnexin, and ATL3 clustered and colocalized with PLN in R14$^{\Delta/\Delta}$ mice, while troponin and Tom20 did not, and comparable results with more clusters were observed at 5 weeks of age (Figure S6 and S7). Similarly, in 18-week-old R14$^{\Delta/\Delta}$DWORF^{Tg} mice, cardiomyocytes that contained large PLN clusters showed colocalization of SERCA2, HRC, calnexin, and ATL3 and with PLN, whereas troponin and Tom20 did not colocalize (Figure S8). These data indicate that more cardiomyocytes develop an abnormal S/ER structure in R14$^{\Delta/\Delta}$ mice with age, and this process is delayed in R14$^{\Delta/\Delta}$DWORF^{Tg} mice.

To corroborate this finding, we investigated the localization of these SR proteins in cardiac tissue from PLN-R14del human patients and non–PLN-R14del dilated cardiomyopathy patients. Perinuclear PLN localization could be observed in some cardiomyocytes in PLN-R14del patient-derived heart tissue, as described previously.[11] Importantly, SERCA2, HRC, calnexin, and ATL3 all colocalized with these PLN clusters in these patient samples (Figure S9), confirming our observations

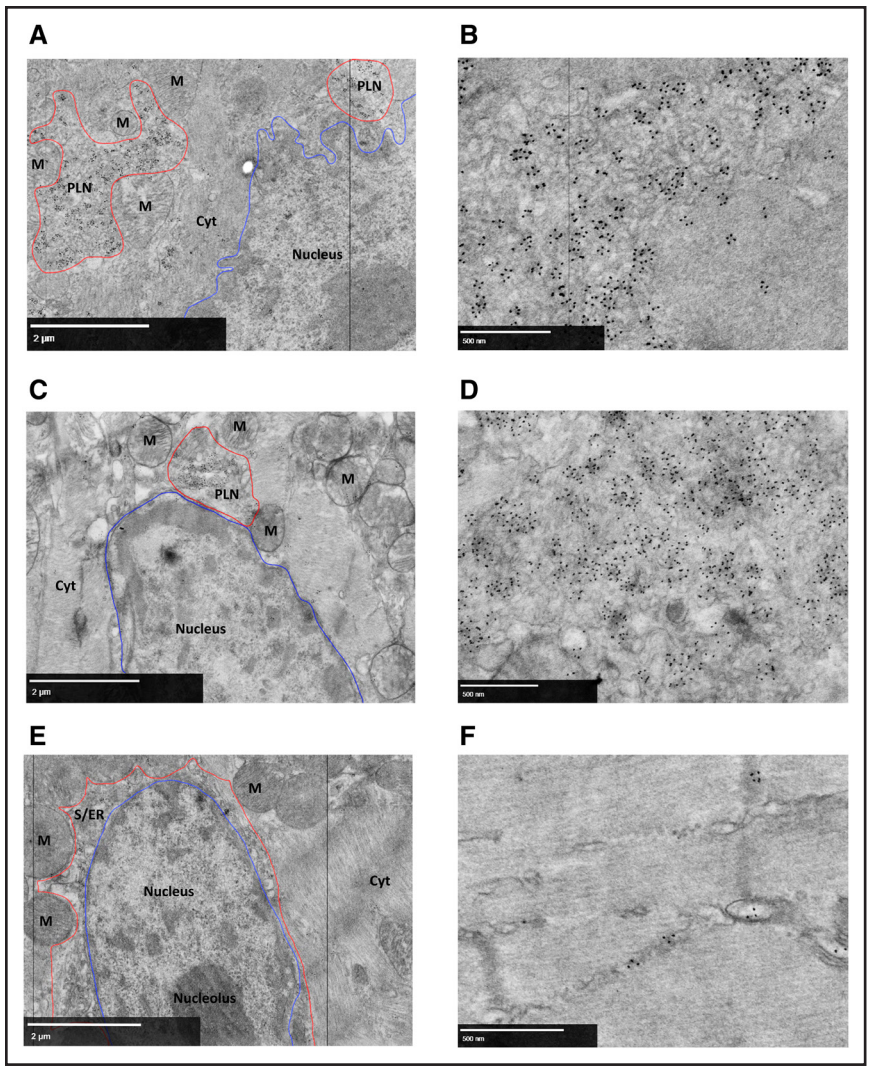

Figure 5. Perinuclear clustering of PLN (phospholamban)-positive membranes in R14$^{\Delta/\Delta}$ (homozygous PLN-R14del) cardiomyocytes. Representative (best illustrative) electron microscopic (EM) images from cardiac tissue labeled for PLN of (**A**) 7-week-old R14$^{\Delta/\Delta}$ mice showing perinuclear PLN clustered signal, with (**B**) a close-up EM image showing PLN quantum dot positive aberrant membrane structures; (**C**) 18-week-old R14$^{\Delta/\Delta}$DWORF^{Tg} (R14$^{\Delta/\Delta}$ mice carrying the DWORF transgene) mice showing perinuclear PLN clustered signal, with (**D**) a close-up EM image showing PLN quantum dot positive aberrant membrane structures; (**E**) 7-week-old wild-type (WT) mice showing perinuclear PLN signal in the sarco/endoplasmic reticulum (S/ER) with (**F**) a close-up of PLN quantum dot positive S/ER. S/ER or PLN-positive membrane clusters outlined in red, and nucleus outlined in blue. Scale bar, 2 µm (**A**, **C**, and **E**) or 500 nm (**B**, **D**, and **F**; n=4 for 7-wk-old WT and R14$^{\Delta/\Delta}$ mice; n=2 for 18-wk-old R14$^{\Delta/\Delta}$DWORF^{Tg} mice). Cyt indicates cytosol; DWORF, dwarf open reading frame; and M, mitochondrion.

in mice. In non–PLN-R14del dilated cardiomyopathy patient-derived cardiac tissue, perinuclear PLN clusters were not observed, and S/ER markers showed a normal distribution in all cardiomyocytes (Figure S10). Taken together, these data confirm perinuclear PLN clustering as a key characteristic of PLN cardiomyopathy and show that these previously identified PLN aggregates are comprised of disorganized S/ER and DWORF overexpression can delay this disorganization.

DWORF Overexpression Delays S/ER Disorganization and Cell Death by Restraining PLN Cluster Size

Closer investigation of abnormal PLN localization revealed that adjacent to cells with large PLN clusters, about 80% of all cardiomyocytes of 18-week-old R14$^{\Delta/\Delta}$DWORF^{Tg} mice showed the presence of small sized PLN speckles (Figure S11, some PLN speckles are indicated by white arrowheads and Figure S12 for quantification). These PLN speckles could also be observed in about 30% of the cardiomyocytes in 3-week-old R14$^{\Delta/\Delta}$ mice, often located next to some cells with larger clusters, suggesting that these speckles represent an initial stage that progresses into larger clusters (Figure S11 and S12). In 7-week-old R14$^{\Delta/\Delta}$DWORF^{Tg} mice, these speckles were much less prevalent compared with 18-week-old R14$^{\Delta/\Delta}$DWORF^{Tg} mice (only in about 30% of all cardiomyocytes), indicating that this phenomenon occurs at a slower rate in the presence of DWORF and develop less frequently into larger clusters (Figures S11 and S12).

Although we currently do not understand how DWORF interferes with these processes, we believe that PLN clustering and SR disorganization have major consequences for cardiomyocyte cell viability. Severe accumulation of the stress-inducible protein, p62, was observed within cardiomyocytes that contain large PLN clusters (Figure 7A). When quantified, R14$^{\Delta/\Delta}$ mice had a significantly higher count of p62-positive cardiomyocytes compared with R14$^{\Delta/\Delta}$DWORF^{Tg} mice (Figure S13). About 10% of the p62-positive cardiomyocytes had p62 accumulation throughout the entire cell together with a strongly reduced signal for the troponin protein, which

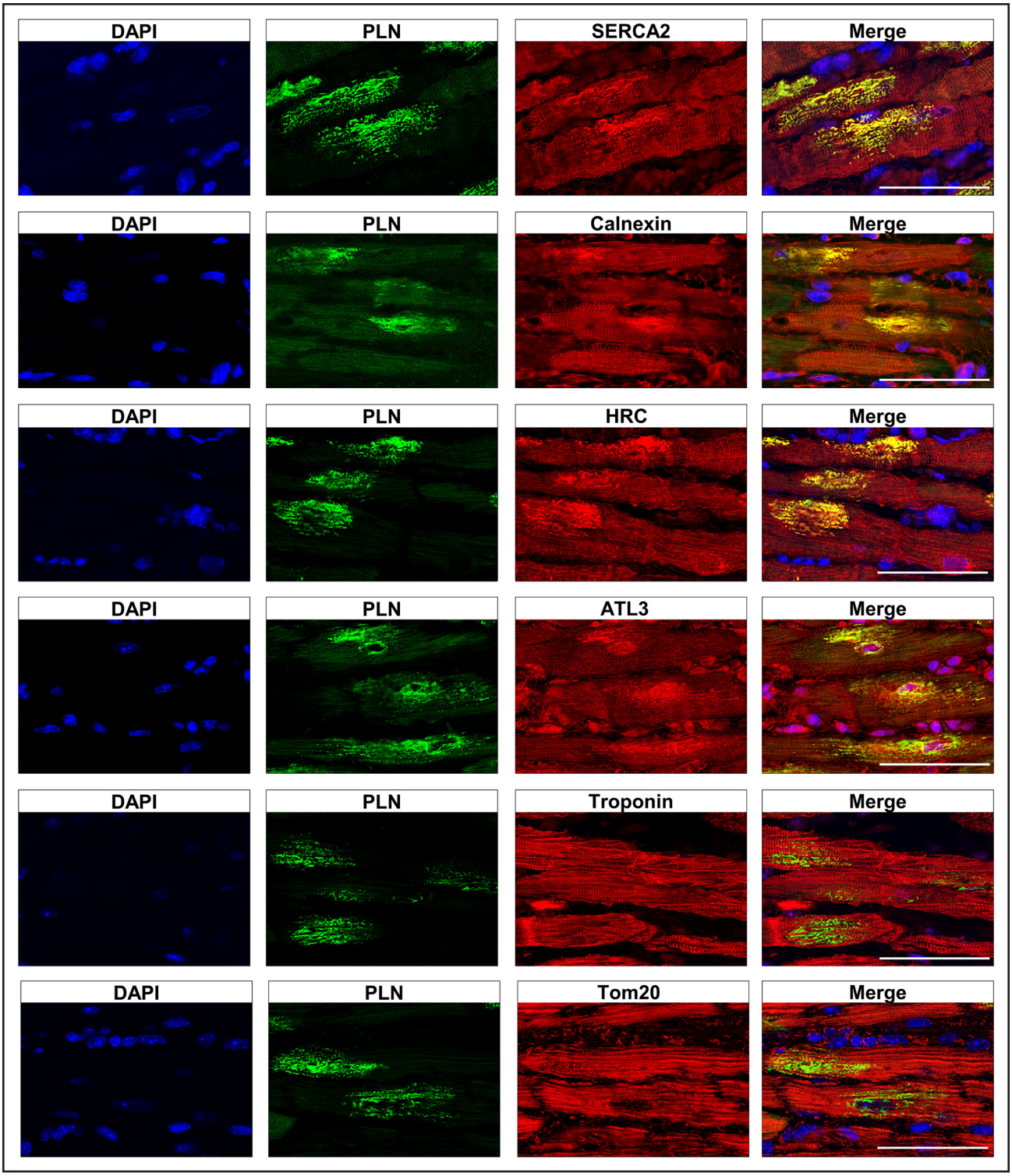

Figure 6. Clustering of sarco/endoplasmic reticulum (S/ER) proteins in R14$^{\Delta/\Delta}$ (homozygous PLN-R14del) cardiomyocytes. Representative (average based) immunofluorescent double staining for PLN (phospholamban) together with SERCA2 (sarco/endoplasmic reticulum Ca^{2+} ATPase 2), calnexin, HRC (histidine-rich calcium binding protein), ATL3 (atlastin-3), troponin, or Tom20 (translocase of outer mitochondrial membrane 20) in left ventricular tissue sections from 7-week-old R14$^{\Delta/\Delta}$ mice (n=6; scale bars, 50 µm).

suggest cardiomyocyte death, most likely by necrosis (Figure 7B; Figure S13B). In vivo Evans blue staining confirmed the presence of necrotic cardiomyocytes in R14$^{\Delta/\Delta}$ mice (Figure 7C and 7D). Consistent with these findings, plasma cardiac troponin levels were strongly elevated in 6-week-old R14$^{\Delta/\Delta}$ mice while skeletal troponin levels remained low, indicative of troponin leakage from the heart (Figure 7E and 7F). Moreover, plasma

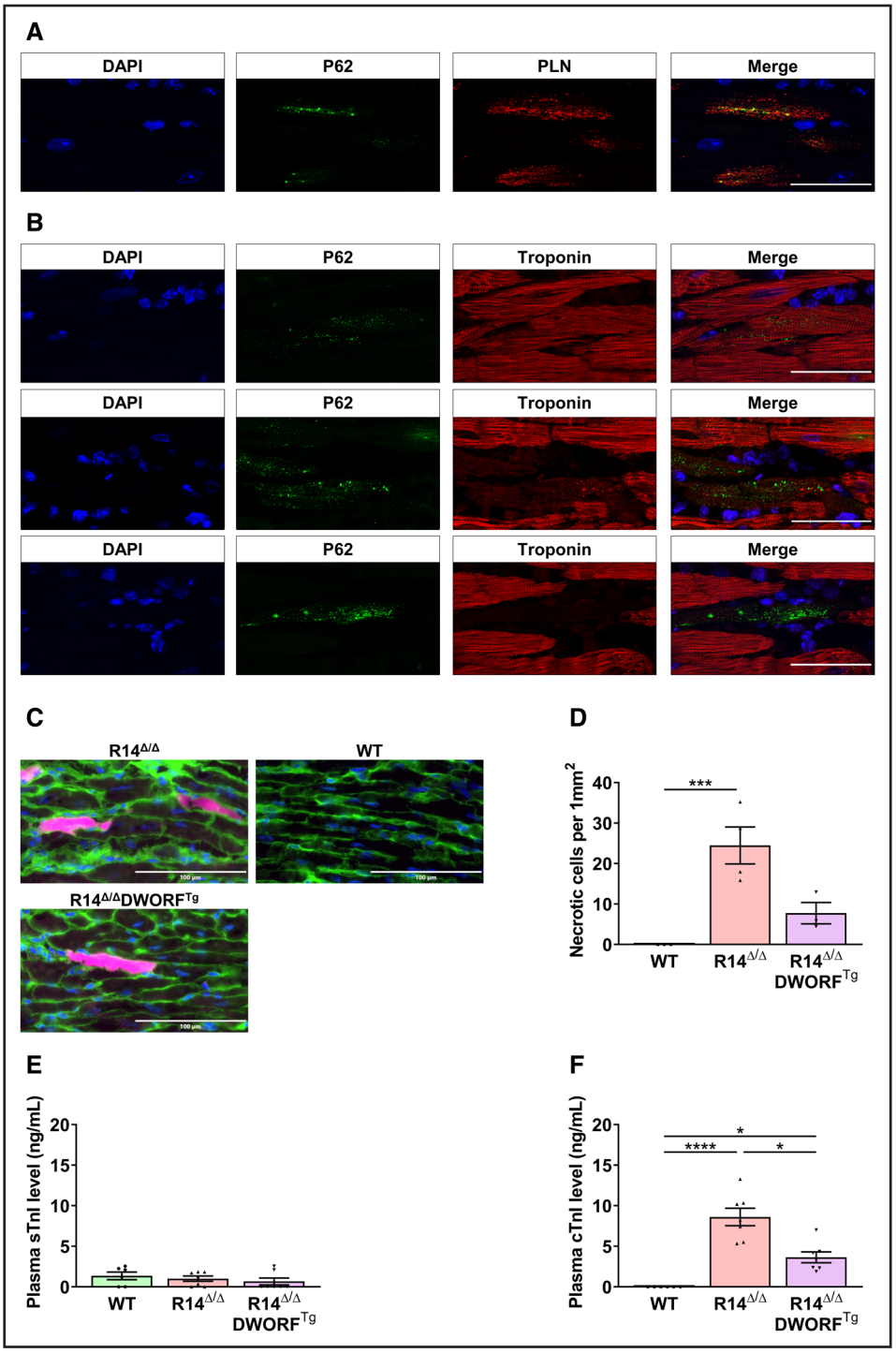

Figure 7. R14$^{\Delta/\Delta}$ (homozygous PLN-R14del) cardiomyocyte cell death.
A, Representative (best illustrative) immunofluorescent (IF) double staining for PLN (phospholamban; red) together with p62 (green) and 4',6-diamidino-2-phenylindole (DAPI; blue) in left ventricular (LV) tissue sections of 7-week-old R14$^{\Delta/\Delta}$ mice. **B**, Representative (best illustrative) IF double staining for troponin (red) together with p62 (green) and DAPI (blue) in LV tissue sections of 7-week-old R14$^{\Delta/\Delta}$ mice (n=4; scale bar, 50 µm). **C**, Representative (average based) images of Evans blue (pink), wheat germ agglutinin (WGA; green), and DAPI (blue) stained hearts from 6-week-old wild-type (WT), R14$^{\Delta/\Delta}$, and R14$^{\Delta/\Delta}$DWORF^{Tg} (R14$^{\Delta/\Delta}$ ice carrying the DWORF transgene) hearts (×35 magnification; scale bar, 100 µm). **D**, Evans blue positive cardiomyocyte count per 1 mm^2 at 6 weeks of age, indicative of cardiomyocyte necrosis occurrence (n=3–4 per group). Skeletal troponin I (**E**) and cardiac troponin I (**F**) levels in plasma of 6-week-old WT, R14$^{\Delta/\Delta}$, and R14$^{\Delta/\Delta}$DWORF^{Tg} mice (n=6–7 per group). Significance was examined by Kruskal-Wallis with Dunn multiple comparisons test. DWORF indicates dwarf open reading frame. *P<0.05, ***P<0.001, ****P<0.0001.

cardiac troponin levels were lower in R14$^{\Delta/\Delta}$DWORF^{Tg} mice compared with R14$^{\Delta/\Delta}$ mice (Figure 7E and 7F). The extensive increase in extracellular matrix in 7-week-old R14$^{\Delta/\Delta}$ mice and 18-week-old R14$^{\Delta/\Delta}$DWORF^{Tg} mice (Figure 2), therefore, most likely reflects replacement fibrosis, which is in agreement with observations in human PLN-R14del cardiomyopathy hearts.[30] Since large PLN-R14del cluster formation is less prominent in R14$^{\Delta/\Delta}$DWORF^{Tg} mice, the delayed cardiac dysfunction and decreased fibrosis can be explained by a reduced rate of cardiomyocyte cell loss in the hearts of R14$^{\Delta/\Delta}$DWORF^{Tg} mice.

DISCUSSION

In this study, we demonstrate that DWORF expression can substantially extend the life span of mice with PLN-R14del cardiomyopathy. DWORF is substantially reduced in HF, and restoration of DWORF levels by crossbreeding DWORF^{Tg} mice with R14$^{\Delta/\Delta}$ mice delayed cardiac dysfunction and fibrosis in these mice. This cardioprotective effect could not be attributed to the role of DWORF in calcium handling. Instead, we provide evidence that characteristic PLN aggregates present in PLN-R14del disease are comprised of harmful perinuclear clustered S/ER and DWORF has an inhibitory effect on this S/ER disorganization, suggesting a novel cardioprotective role of DWORF in PLN-R14del cardiomyopathy.

We show for the first time that the previously termed perinuclear PLN aggregates, observed in both patients and mice with PLN-R14del cardiomyopathy, are not only composed of PLN protein but are comprised of aberrantly clustered cardiac S/ER. Using electron microscopy, we revealed perinuclear localized PLN-dense membrane clusters in hearts of R14$^{\Delta/\Delta}$ mice. Further investigations showed that other S/ER markers, including SERCA2, calnexin, HRC, and ATL3, all colocalized with PLN in these membrane clusters in both R14$^{\Delta/\Delta}$ mouse and PLN-R14del human patient samples. These findings provide clear evidence that in both mice and men, PLN-R14del–induced S/ER disorganization is a major characteristic of PLN-R14del cardiomyopathy. So far, the mechanistic aspects of this abnormal S/ER clustering remain elusive. Further investigations will be needed to investigate whether this process involves abnormal PLN-R14del membrane interactions or PLN aggregation and complex formation with other proteins in the SR membrane.

In addition to the occurrence of abnormal perinuclear PLN clusters in cardiomyocytes before the onset of cardiac dysfunction,[13] our data indicate that cluster formation involves a sequence of events. At an early stage, when the majority of both PLN and S/ER distribution is still normal, the first PLN speckles can be observed in cardiomyocytes. At a later stage, these speckles formed larger PLN clusters and caused severe disorganization of the S/ER. Concurrently, p62 accumulation was observed in about half of the cardiomyocytes with large PLN clusters. Importantly, in about 10% of the cardiomyocytes with p62 cluster formation, troponin was strongly reduced, which was accompanied by an increase in plasma troponin levels, which collectively indicates necrotic death of these cardiomyocytes. These results were further confirmed by injection of Evans blue, a previously described necrotic cell death marker,[31] and are again in line with the high vulnerability of these cardiomyocytes during isolation. This also explains the excessive replacement fibrosis in these hearts and concomitant development of hypertrophy in the remaining cardiomyocytes and is in congruence with the cell death–fibrosis phenomenon in HF.[32] Importantly, in PLN-R14del mutation carriers, fibrosis is an early feature, which can already be observed in carriers that still have a preserved LVEF.[33] Thus, although the exact molecular processes require further investigations, our observations indicate that abnormal perinuclear S/ER cluster formation is an early phenomenon that drives a sequence of pathological processes resulting in PLN-R14del cardiomyopathy.

Interestingly, DWORF overexpression inhibited the presence of large perinuclear PLN clusters with severe S/ER disorganization in R14$^{\Delta/\Delta}$ mice. At 3 weeks of age the majority of the R14$^{\Delta/\Delta}$DWORF^{Tg} cardiomyocytes showed normal PLN distribution, and at 18 weeks of age, the majority of the R14$^{\Delta/\Delta}$DWORF^{Tg} cardiomyocytes have PLN speckles. By restraining PLN cluster size and inhibiting the formation of large perinuclear PLN clusters, that are associated with cardiomyocyte death, DWORF overexpression could delay disease development in R14$^{\Delta/\Delta}$ mice. Currently, we do not know how DWORF mediates PLN cluster size, but since SERCA is present in these clusters as well, it may still involve some form of competitive SERCA interactions. The knowledge about the regulation and associations of PLN and other micropeptides, like DWORF, in biological membranes is still limited, but sophisticated technologies like electron paramagnetic resonance spectroscopy might provide answers to this underlying complexity.[34] Other mechanisms, like control of dynamic localization via neprilysin-mediated changes in oligomerization states, as shown for *Drosophila* sarcolamban should not be excluded, although our results currently do not point into this direction.[35] Unfortunately, the absence of a DWORF antibody for histological investigations does currently not allow us to investigate the presence of DWORF in these S/ER clusters. Despite strong reduction in PLN S/ER cluster formations, cells with clusters still develop and were also observed in 7- and 18-week-old R14$^{\Delta/\Delta}$DWORF^{Tg} mice. This reduced rate of detrimental cluster formation can explain the strongly delayed deterioration of cardiac function of R14$^{\Delta/\Delta}$DWORF^{Tg} mice overtime (Figure S14).

Studies with the PLN-R14del pathogenic variant have repeatedly shown altered calcium handling properties, but

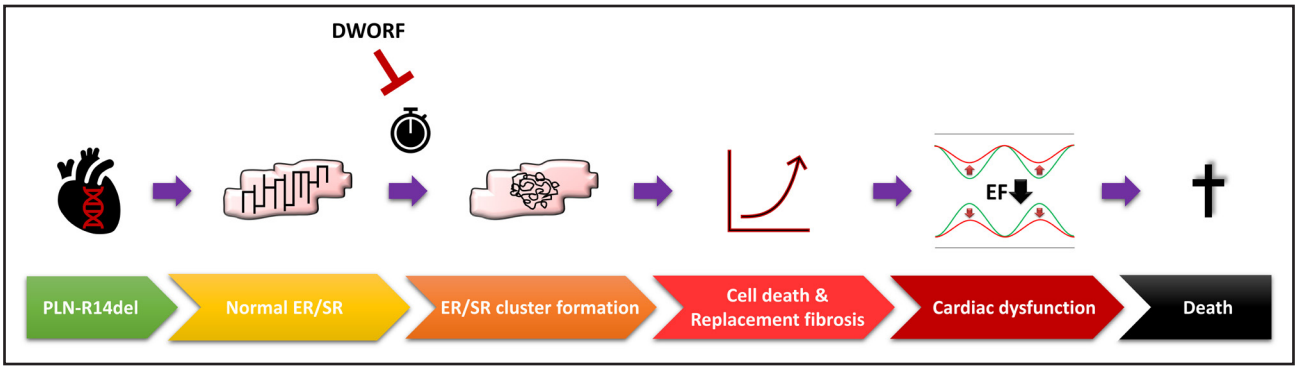

Figure 8. The proposed new view on PLN-R14del cardiomyopathy with respect to sarco/endoplasmic reticulum (S/ER) cluster formation and the interference of dwarf open reading frame (DWORF).
EF indicates ejection fraction; PLN, phospholamban; and SR, sarcoplasmic reticulum.

the exact effects and mechanisms remain unclear.[4–7,10,13,36] Here, we described enhanced calcium reuptake in cardiomyocytes isolated from R14$^{\Delta/\Delta}$ mice, which is in line with several other publications on altered calcium reuptake by mutant PLN-R14del.[6–8,36] Likewise, calcium S/ER reuptake is accelerated in PLN$^{-/-}$ (knockout) mice, but in contrast to R14$^{\Delta/\Delta}$ mice, PLN knockout mice do not develop HF.[37,38] Thus, the p.Arg14del pathogenic variant may behave as a loss-of-function mutation in calcium handling, but this cannot explain disease development in R14$^{\Delta/\Delta}$ mice. Since calcium reuptake was already enhanced in R14$^{\Delta/\Delta}$ cardiomyocytes, DWORF overexpression did not result in an additional increase in calcium reuptake in R14$^{\Delta/\Delta}$DWORF^{Tg} cardiomyocytes. Hence, improving calcium S/ER reuptake appears to be ineffective in PLN-R14del cardiomyopathy. Therefore, in contrast to the protective effects of DWORF in other HF models,[14,17,39] its protective effect in PLN-R14del cardiomyopathy does not appear to be related to calcium handling. Based on the data presented above, we, therefore, consider it more likely that the protective effect of DWORF involves the prevention of abnormal S/ER cluster formation in PLN-R14del cardiomyopathy.

A limitation of this study is that we did not use a heterozygous PLN-R14del mouse model (R14$^{+/\Delta}$), which would resemble the same genetic situation as human carriers with 1 normal and 1 pathogenic allele. Instead, we used an R14$^{\Delta/\Delta}$ mouse model that shows similar characteristics as the R14$^{+/\Delta}$ mice and human patients but has the advantage of accelerated disease development. In addition to previously published data, we confirmed that the R14$^{+/\Delta}$ mouse model is a mild disease variant with regard to calcium handling and sarcomere function. Relaxation is also accelerated in adult cardiomyocytes from R14$^{+/\Delta}$ mice, with relaxation time and velocity values intermediate of R14$^{\Delta/\Delta}$ and WT mice (Figure S15). Moreover, our finding that perinuclear PLN structures are composed of disorganized S/ER in homozygous mice was confirmed in PLN-R14del patient tissue, which further validates the translatability of this mouse model. The strategy of increasing the DWORF level to delay disease progression could be even more effective in human patients compared with the effects observed in the current study in homozygous mice, considering that disease progression is milder due to the presence of WT PLN in patients.

In summary, PLN-R14del–induced perinuclear clustering of PLN and S/ER structural deformations trigger cardiomyocyte dysfunction. This causes cardiomyocyte cell loss as indicated by elevated troponin levels, explaining the excessive fibrosis, which finally culminates in severe cardiac dysfunction and death (Figure 8). Whether other PLN pathogenic variants also cause structural S/ER alterations is not known but deserves future attention. Importantly, DWORF can diminish PLN-R14del–induced S/ER cluster formation and significantly extend life span in an established mouse model for PLN-R14del cardiomyopathy (Figure 8).

To conclude, we reveal that the characteristic PLN clusters present in the PLN-R14del mouse model and human patients are comprised of disorganized perinuclear S/ER and argue that aberrant S/ER formation is the key mechanism in the development of PLN-R14del cardiomyopathy. Preventing structural S/ER alterations by DWORF overexpression or by other interventions could be a promising therapeutic strategy in this disease.

ARTICLE INFORMATION

Received June 30, 2023; revision received October 18, 2023; accepted November 1, 2023.

Affiliations

Department of Cardiology, University Medical Center Groningen, University of Groningen, the Netherlands (N.M.S., T.R.E., V.O.N.T., A.M.F., E.M.S., R.A.d.B., H.H.W.S.). Department of Physiology (D.W.D.K., J.v.d.V.) and Amsterdam Cardiovascular Sciences, Heart Failure and Arrhythmias (D.W.D.K., J.v.d.V.), Amsterdam UMC, Vrije Universiteit Amsterdam, the Netherlands. Biomedical Sciences of Cells and Systems, UMC Groningen, University of Groningen, the Netherlands (A.H.G.W., B.N.G.G.). Division of Molecular Cardiovascular Biology of the Heart Institute, Cincinnati Children's Hospital Medical Center, OH (C.A.M.). Department of Pediatrics, University of Cincinnati College of Medicine, OH (C.A.M.). Department of Molecular Biology and

Hamon Center for Regenerative Science and Medicine, University of Texas Southwestern Medical Center, Dallas (R.B.-D., E.N.O.). Department of Cardiology, Erasmus University Medical Center, Rotterdam, the Netherlands (R.A.d.B.).

Acknowledgments

The authors would like to thank Sietske-Nyncke Zijlstra and Martin M. Dokter for their excellent technical assistance with, among others, the calcium contraction assays performed on isolated adult mouse cardiomyocytes and histological analyses. Moreover, they are grateful for the human patient tissues that have been retrieved from the UMCG Pathology Biobank and would like to thank animal caretakers and staff from the UMCG central animal facility (CDP) for their services.

Sources of Funding

This work was supported by a grant from the Netherlands Heart Foundation (CVON PREDICT2, grant 2018-30), the Leducq Foundation (Cure Phospholamban Induced Cardiomyopathy), the Ubbo Emmius Foundation, grants from the Netherlands Heart Institute, the PLN Foundation, the European Research Council (ERC CoG 818715, SECRETE-HF to R.A. de Boer), the National Institutes of Health grants (HL130253 to R. Bassel-Duby and E.N. Olson; HL141630 to C.A. Makarewich), Leducq Foundation Transatlantic Network of Excellence (20CVD04 to E.N. Olson), ZonMW grant (91111.006 to B.N.G. Giepmans), the Netherlands Electron Microscopy Infrastructure to B.N.G. Giepmans, and the Nederlandse Organisatie voor Wetenschappelijk Onderzoek grant (NWO National Roadmap for Large-Scale Research Infrastructure of the Dutch Research Council, 184.034.014 to B.N.G. Giepmans). Part of the work has been performed in the UMCG Microscopy and Imaging Center, sponsored by the Dutch Research Council NWO 175-010-2009-023 and NRGWI.obrug.005.

Disclosures

The UMCG, which employs several of the authors, has received research grants and fees from AstraZeneca, Abbott, Boehringer Ingelheim, Cardior Pharmaceuticals GmbH, Ionis Pharmaceuticals, Inc, Novo Nordisk, and Roche. R.A. de Boer received speaker fees from Abbott, AstraZeneca, Bayer, Novartis, and Roche. The other authors report no conflicts.

Supplemental Material

Supplemental Methods
Tables S1–S4
Figures S1–S15
References 11,12,14,19,29
Statistical Report

REFERENCES

1. Van Der Zwaag PA, Van Rijsingen IAW, Asimaki A, Jongbloed JDH, Van Veldhuisen DJ, Wiesfeld ACP, Cox MGPJ, Van Lochem LT, De Boer RA, Hofstra RMW, et al. Phospholamban R14del mutation in patients diagnosed with dilated cardiomyopathy or arrhythmogenic right ventricular cardiomyopathy: evidence supporting the concept of arrhythmogenic cardiomyopathy. *Eur J Heart Fail.* 2012;14:1199–1207. doi: 10.1093/eurjhf/hfs119
2. Hof IE, van der Heijden JF, Kranias EG, Sanoudou D, de Boer RA, van Tintelen JP, van der Zwaag PA, Doevendans PA. Prevalence and cardiac phenotype of patients with a phospholamban mutation. *Netherlands Hear J.* 2019;27:64–69. doi: 10.1007/s12471-018-1211-4
3. MacLennan DH, Kranias EG. Phospholamban: a crucial regulator of cardiac contractility. *Nat Rev Mol Cell Biol.* 2003;4:566–577. doi: 10.1038/nrm1151
4. Haghighi K, Kolokathis F, Gramolini AO, Waggoner JR, Pater L, Lynch RA, Fan GC, Tsiapras D, Parekh RR, Dorn GW, et al. A mutation in the human phospholamban gene, deleting arginine 14, results in lethal, hereditary cardiomyopathy. *Proc Natl Acad Sci USA.* 2006;103:1388–1393. doi: 10.1073/pnas.0510519103
5. Kumar M, Haghighi K, Koch S, Rubinstein J, Stillitano F, Hajjar RJ, Kranias EG, Sadayappan S. Myofilament alterations associated with human R14del-phospholamban cardiomyopathy. *Int J Mol Sci.* 2023;24:2675. doi: 10.3390/ijms24032675
6. Ceholski DK, Trieber CA, Young HS. Hydrophobic imbalance in the cytoplasmic domain of phospholamban is a determinant for lethal dilated cardiomyopathy. *J Biol Chem.* 2012;287:16521–16529. doi: 10.1074/jbc.M112.360859
7. Badone B, Ronchi C, Lodola F, Knaust AE, Hansen A, Eschenhagen T, Zaza A. Characterization of the PLN pArg14del mutation in human induced pluripotent stem cell-derived cardiomyocytes. *Int J Mol Sci.* 2021;22:13500. doi: 10.3390/ijms222413500
8. Haghighi K, Pritchard T, Bossuyt J, Waggoner JR, Yuan Q, Fan GC, Osinska H, Anjak A, Rubinstein J, Robbins J, et al. The human phospholamban Arg14-deletion mutant localizes to plasma membrane and interacts with the Na/K-ATPase. *J Mol Cell Cardiol.* 2012;52:773–782. doi: 10.1016/j.yjmcc.2011.11.012
9. Wu AZ, Xu D, Yang N, Lin SF, Chen PS, Cala SE, Chen Z. Phospholamban is concentrated in the nuclear envelope of cardiomyocytes and involved in perinuclear/nuclear calcium handling. *J Mol Cell Cardiol.* 2016;100:1–8. doi: 10.1016/j.yjmcc.2016.09.008
10. Cuello F, Knaust AE, Saleem U, Loos M, Raabe J, Mosqueira D, Laufer S, Schweizer M, Kraak P, Flenner F, et al. Impairment of the ER/mitochondria compartment in human cardiomyocytes with PLN pArg14del mutation. *EMBO Mol Med.* 2021;13:e13074. doi: 10.15252/emmm.202013074
11. te Rijdt WP, van Tintelen JP, Vink A, van der Wal AC, de Boer RA, van den Berg MP, Suurmeijer AJH. Phospholamban pArg14del cardiomyopathy is characterized by phospholamban aggregates, aggresomes, and autophagic degradation. *Histopathology.* 2016;69:542–550. doi: 10.1111/his.12963
12. Eijgenraam TR, Boukens BJ, Boogerd CJ, Schouten EM, van de Kolk CWA, Stege NM, te Rijdt WP, Hoorntje ET, van der Zwaag PA, van Rooij E, et al. The phospholamban p(Arg14del) pathogenic variant leads to cardiomyopathy with heart failure and is unresponsive to standard heart failure therapy. *Sci Rep.* 2020;10:9819. doi: 10.1038/s41598-020-66656-9
13. Eijgenraam TR, Boogerd CJ, Stege NM, Oliveira Nunes Teixeira V, Dokter MM, Schmidt LE, Yin X, Theofilatos K, Mayr M, van der Meer P, et al. Protein aggregation is an early manifestation of phospholamban p(Arg14del)-related cardiomyopathy: development of PLN-R14del-related cardiomyopathy. *Circ. Heart Fail.* 2021;14:e008532. doi: 10.1161/CIRCHEARTFAILURE.121.008532
14. Nelson BR, Makarewich CA, Anderson DM, Winders BR, Troupes CD, Wu F, Reese AL, McAnally JR, Chen X, Kavalali ET, et al. Muscle physiology: a peptide encoded by a transcript annotated as long noncoding RNA enhances SERCA activity in muscle. *Science.* 2016;351:271–275. doi: 10.1126/science.aad4076
15. Fisher ME, Bovo E, Cho EE, Pribadi MP, Dalton MP, Lemieux MJ, Rathod N, Aguayo-Ortiz R, Espinoza-Fonseca LM, Robia SL, et al. Dwarf open reading frame (DWORF) peptide is a direct activator of the sarcoplasmic reticulum calcium pump SERCA. *bioRxiv.* 2020;10:e65545. doi: 10.7554/eLife.65545
16. Li A, Yuen SL, Stroik DR, Kleinboehl E, Cornea RL, Thomas DD. The transmembrane peptide DWORF activates SERCA2a via dual mechanisms. *J Biol Chem.* 2021;296:100412. doi: 10.1016/j.jbc.2021.100412
17. Makarewich CA, Munir AZ, Schiattarella GG, Bezprozvannaya S, Raguimova ON, Cho EE, Vidal AH, Robia SL, Bassel-Duby R, Olson EN. The DWORF micropeptide enhances contractility and prevents heart failure in a mouse model of dilated cardiomyopathy. *Elife.* 2018;7:e38319. doi: 10.7554/eLife.38319
18. Makarewich CA, Bezprozvannaya S, Gibson AM, Bassel-Duby R, Olson EN. Gene therapy with the DWORF micropeptide attenuates cardiomyopathy in mice. *Circ Res.* 2020;127:1340–1342. doi: 10.1161/CIRCRESAHA.120.317156
19. Du W, Piek A, Marloes Schouten E, van de Kolk CWA, Mueller C, Mebazaa A, Voors AA, de Boer RA, Silljé HHW. Plasma levels of heart failure biomarkers are primarily a reflection of extracardiac production. *Theranostics.* 2018;8:4115. doi: 10.7150/thno.26055
20. du Sert NP, Hurst V, Ahluwalia A, Alam S, Avey MT, Baker M, Browne WJ, Clark A, Cuthill IC, Dirnagl U, et al. The ARRIVE guidelines 20: updated guidelines for reporting animal research. *PLoS Biol.* 2020;18:e3000410. doi: 10.1371/journal.pbio.3000410
21. Withaar C, Meems LMG, Markousis-Mavrogenis G, Boogerd CJ, Silljé HHW, Schouten EM, Dokter MM, Voors AA, Westenbrink BD, Lam CSP, et al. The effects of liraglutide and dapagliflozin on cardiac function and structure in a multi-hit mouse model of heart failure with preserved ejection fraction. *Cardiovasc Res.* 2021;117:2108–2124. doi: 10.1093/cvr/cvaa256
22. Zacchigna S, Paldino A, Falcão-Pires I, Daskalopoulos EP, Dal Ferro M, Vodret S, Lesizza P, Cannatà A, Miranda-Silva D, Lourenço AP, et al. Towards standardization of echocardiography for the evaluation of left ventricular function in adult rodents: a position paper of the ESC Working Group on Myocardial Function. *Cardiovasc Res.* 2021;117:43–59. doi: 10.1093/cvr/cvaa110
23. Schneider CA, Rasband WS, Eliceiri KW. NIH image to ImageJ: 25 years of image analysis. *Nat Methods.* 2012;9:671–675. doi: 10.1038/nmeth.2089
24. Ackers-Johnson M, Li PY, Holmes AP, O'Brien SM, Pavlovic D, Foo RS. A simplified, langendorff-free method for concomitant isolation of viable cardiac myocytes and nonmyocytes from the adult mouse heart. *Circ Res.* 2016;119:909–920. doi: 10.1161/CIRCRESAHA.116.309202

25. de Boer P, Pirozzi NM, Wolters AHG, Kuipers J, Kusmartseva I, Atkinson MA, Campbell-Thompson M, Giepmans BNG. Large-scale electron microscopy database for human type 1 diabetes. *Nat Commun*. 2020;11:2475. doi: 10.1038/s41467-020-16287-5
26. Kuipers J, de Boer P, Giepmans BNG. Scanning EM of non-heavy metal stained biosamples: large-field of view, high contrast and highly efficient immunolabeling. *Exp Cell Res*. 2015;337:202–207. doi: 10.1016/j.yexcr.2015.07.012
27. Sikkel MB, Francis DP, Howard J, Gordon F, Rowlands C, Peters NS, Lyon AR, Harding SE, Macleod KT. Hierarchical statistical techniques are necessary to draw reliable conclusions from analysis of isolated cardiomyocyte studies. *Cardiovasc Res*. 2017;113:1743–1752. doi: 10.1093/cvr/cvx151
28. Grote Beverborg N, Später D, Knöll R, Hidalgo A, Yeh ST, Elbeck Z, Silljé HHW, Eijgenraam TR, Siga H, Zurek M, et al. Phospholamban antisense oligonucleotides improve cardiac function in murine cardiomyopathy. *Nat Commun*. 2021;12:5180. doi: 10.1038/s41467-021-25439-0
29. te Rijdt WP, van der Klooster ZJ, Hoorntje ET, Jongbloed JDH, van der Zwaag PA, Asselbergs FW, Dooijes D, de Boer RA, van Tintelen JP, van den Berg MP, et al. Phospholamban immunostaining is a highly sensitive and specific method for diagnosing phospholamban pArg14del cardiomyopathy. *Cardiovasc Pathol*. 2017;30:23–26. doi: 10.1016/j.carpath.2017.05.004
30. Eijgenraam TR, Silljé HHW, de Boer RA. Current understanding of fibrosis in genetic cardiomyopathies. *Trends Cardiovasc Med*. 2020;30:353. doi: 10.1016/j.tcm.2019.09.003
31. Nickel AG, Von Hardenberg A, Hohl M, Löffler JR, Kohlhaas M, Becker J, Reil JC, Kazakov A, Bonnekoh J, Stadelmaier M, et al. Reversal of mitochondrial transhydrogenase causes oxidative stress in heart failure. *Cell Metab*. 2015;22:472–484. doi: 10.1016/j.cmet.2015.07.008
32. Piek A, de Boer RA, Silljé HHW. The fibrosis-cell death axis in heart failure. *Heart Fail Rev*. 2016;21:199–211. doi: 10.1007/s10741-016-9536-9
33. Te Rijdt WP, Ten Sande JN, Gorter TM, Van Der Zwaag PA, Van Rijsingen IA, Boekholdt SM, Van Tintelen JP, Van Haelst PL, Planken RN, De Boer RA, et al. Myocardial fibrosis as an early feature in phospholamban p.Arg14del mutation carriers: phenotypic insights from cardiovascular magnetic resonance imaging. *Eur Heart J Cardiovasc Imaging*. 2019;20:92–100. doi: 10.1093/ehjci/jey047
34. Rustad MD, Roopnarine O, Cornea RL, Thomas DD. Interaction of DWORF with SERCA and PLB as determined by EPR spectroscopy. *Biochem Biophys Res Commun*. 2023;645:97–102. doi: 10.1016/j.bbrc.2023.01.041
35. Schiemann R, Buhr A, Cordes E, Walter S, Heinisch JJ, Ferrero P, Milting H, Paululat A, Meyer H. Neprilysins regulate muscle contraction and heart function via cleavage of SERCA-inhibitory micropeptides. *Nat Commun*. 2022;13:4420. doi: 10.1038/s41467-022-31974-1
36. Hughes E, Middleton DA. Comparison of the structure and function of phospholamban and the arginine-14 deficient mutant associated with dilated cardiomyopathy. *PLoS One*. 2014;9:e106746. doi: 10.1371/journal.pone.0106746
37. Luo W, Grupp IL, Harrer J, Ponniah S, Grupp G, Duffy JJ, Doetschman T, Kranias EG. Targeted ablation of the phospholamban gene is associated with markedly enhanced myocardial contractility and loss of beta-agonist stimulation. *Circ Res*. 1994;75:401–409. doi: 10.1161/01.res.75.3.401
38. Slack JP, Grupp IL, Dash R, Holder D, Schmidt A, Gerst MJ, Tamura T, Tilgmann C, James PF, Johnson R, et al. The enhanced contractility of the phospholamban-deficient mouse heart persists with aging. *J Mol Cell Cardiol*. 2001;33:1031–1040. doi: 10.1006/jmcc.2001.1370
39. Morales ED, Yue Y, Watkins TB, Han J, Pan X, Gibson AM, Hu B, Brito-Estrada O, Yao G, Makarewich CA, et al. Dwarf open reading frame (DWORF) gene therapy ameliorated duchenne muscular dystrophy cardiomyopathy in aged mdx mice. *J Am Heart Assoc*. 2023;12:e027480. doi: 10.1161/JAHA.122.027480